

Characterization of Chiral H and J Aggregates of Cyanine Dyes Formed by DNA Templating Using Stark and Fluorescence Spectroscopies

Arindam Chowdhury, Sebastian Wachsmann-Hogiu,[†] Prakriti R. Bangal, Izzat Raheem, and Linda A. Peteanu*

Department of Chemistry, Carnegie Mellon University, Pittsburgh, Pennsylvania 15213

Received: July 23, 2001; In Final Form: September 11, 2001

A series of studies is presented to characterize the photophysical properties of a novel type of aggregate formed by the spontaneous noncovalent assembly of numerous cofacial dimers of cyanine dyes (DiSC₃₊(5)) to the minor groove of poly(dI–dC) DNA. The dimensions of these helical aggregates, first synthesized and characterized by Armitage and co-workers (*J. Am. Chem. Soc.* **2000**, *122*, 9977–9986), are restricted to the width of the dye dimer because of steric constraints in the minor groove, though the length of the aggregate can extend essentially for the full length of the DNA template. These unique species exhibit both H- and J-type absorption bands that are shifted from the absorption maximum of the monomeric dye by +1650 and –1275 cm⁻¹, respectively, because of the stacking interactions between the dyes composing the dimers. Additional splittings are seen because of head-to-head interactions between adjacent dye dimers. Here, we present the low-temperature (77 K) absorption, fluorescence, and electroabsorption spectra of these aggregates as well as measurements of the fluorescence lifetime of the monomer and of the J-type emission at 10 °C. The electroabsorption measurements yield values of the average difference polarizability on excitation, $\langle\Delta\alpha\rangle$, for the H and J bands of –74 and –34 Å³, respectively. These are between 2 and 6 times larger than that of the monomer. Both bands exhibit similar values for the difference dipole moment on excitation ($|\Delta\mu|$) of between 0.6 and 0.7 D that are somewhat smaller than that of the monomer (1.1 D). The absorption and fluorescence experiments show that the line width of the J band is ~4 times narrower than the experimental fwhm of the DiSC₃₊(5) monomer while the fluorescence decay of the aggregate is roughly a factor of 2 faster. Implications of all of these measurements for determining the number of dyes that are excited cooperatively upon light absorption are discussed.

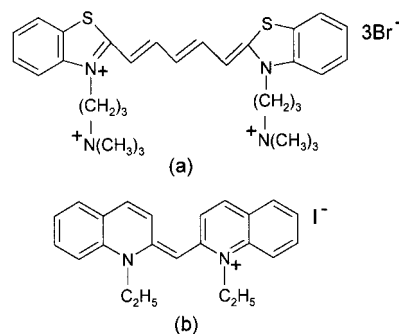
Introduction

Molecular aggregates are important to materials science, chemistry,¹ and light-harvesting biological systems.² Dye aggregates bound by noncovalent interactions are frequently used as photographic sensitizers³ and are predicted to have strong nonlinear optical responses.⁴

Many of the unique properties of aggregates arise from the fact that the constituent molecules are strongly electronically coupled so that optical excitation of the chromophore produces a state that is delocalized over several monomer units. In fluorescent aggregates, this coherent coupling produces the phenomenon of superradiance (fluorescence intensity scaling with N where N is the number of coupled chromophores), which is useful from the standpoint of optical imaging and laser development.^{5–9} Likewise, delocalization of the initial excitation frequently causes aggregates to have line widths that are considerably narrower than their constituent monomers (motional narrowing), making them attractive for high-density information storage.^{10,11}

Recently, Armitage and co-workers have shown that the spontaneous noncovalent assembly of cyanine dyes such as DiSC₃₊(5) (Chart 1a) within the minor groove of double-stranded DNA creates helical dye aggregates the size and shape

CHART 1: The Cyanine Dyes (a) DiSC₃₊(5) and (b) PIC



of which are defined by the DNA template.^{12,13} Their model for the formation of these structures can be summarized as follows. These dyes initially bind to the minor groove of the DNA as face-to-face dimers because the walls of the groove restrict further expansion (formation of stacked trimers, etc.) along this direction. Binding of a pair of dyes in the minor groove forces the groove to widen, making it energetically favorable for a second pair of dyes to bind adjacent to the first dimer along the long axis of the minor groove. Cooperative assembly of multiple dyes results in the formation of helical dye aggregates that exhibit large circular dichroism (CD) signals, indicative of right-handed chirality. For a detailed discussion of the structure of DNA–dye aggregates, see refs 12 and 13.

One important advantage of this class of aggregates is that, unlike those assembled in solution, their structure and potentially

* To whom correspondence should be addressed. E-mail: peteanu@andrew.cmu.edu.

[†] On leave from the National Institute of Laser, Plasma, and Radiation Physics, Bucharest-Magurele, Romania.

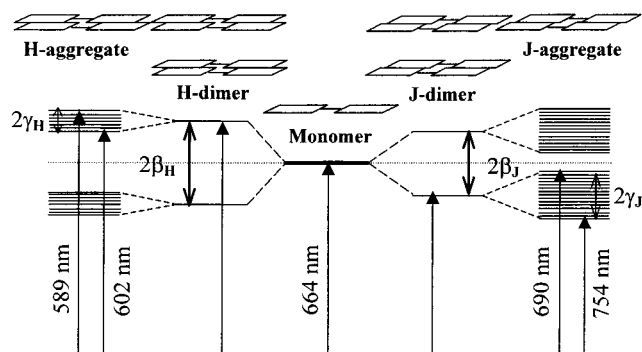


Figure 1. A proposed energy level scheme for H and J aggregates of $\text{DiSC}_{3+}(5)$ formed by noncovalent binding to duplex DNA. The primary splitting (β_H and β_J) that results from the stacking interaction between cyanine dimers and the secondary splitting (γ_H and γ_J) arising from end-to-end interactions between dimers along the length of the H and J aggregates are shown. These interactions are shown schematically above with the rectangles representing the $\text{DiSC}_{3+}(5)$ monomer. Figure adapted from ref 13.

their size can be controlled by the properties of the DNA template used to form them through the binding mechanism described above. Our initial studies, presented here, were performed on $\text{DiSC}_{3+}(5)$ bound to a polymeric strand of DNA (see Experimental Section). As a result, the length of the aggregates formed is not known exactly. However, work is ongoing toward the goal of creating aggregates of well-defined length using DNA oligomers.

A second unique feature of $\text{DiSC}_{3+}(5)$ aggregates bound to DNA is that their absorption and CD spectra show transitions characteristic of both H- and J-type aggregates. A schematic energy level diagram, adapted from ref 13, that illustrates how H- and J-type transitions arise from the excitonic interactions between electronically coupled chromophores is shown in Figure 1. For the aggregates studied here, it is presumed that the face-to-face interaction of the dyes in the minor groove produces the primary energy splitting of the monomer level. This generates two bands, with the upper one being an allowed transition from the ground state for an H-type structure while the lower level is allowed for the J-type species. Their positions relative to the monomer are denoted as β_H and β_J , respectively, in Figure 1. An important consequence of this energy level structure is that only the J-type structure is fluorescent. Additional, weaker splittings are seen in both the H- and J-type bands because of end-to-end interactions between dimers along the length of the aggregate. These are denoted γ_H and γ_J in Figure 1.

One possible reason that both H-type and J-type transitions have been seen in $\text{DiSC}_{3+}(5)$ aggregates bound to DNA is that both types of structures (shown schematically in Figure 1) are present as distinct subpopulations within the sample or that they exist in equilibrium. The latter is thought to be the case for aggregates at room temperature, though it is unlikely at low temperatures.¹³ Armitage et al. have suggested that, at lower temperature (5–30 °C), a single type of aggregate is formed the unique structure of which, imposed by binding to the DNA, makes optical transitions to both the H and J levels from the ground-state allowed.¹³ However, fluorescence excitation spectra, presented below, argue for the presence of distinct populations of H and J aggregates under the conditions of temperature and solvent used in our experiments.

In this study, we investigate the electronic properties of both the H- and J-type transitions arising from $\text{DiSC}_{3+}(5)$ molecules bound to DNA using low-temperature (77 K) absorption, electroabsorption (Stark), and fluorescence spectroscopies. Elec-

troabsorption yields the absolute value of the difference dipole moment on excitation ($|\Delta\mu|$), as well as the average value of the difference polarizability ($\langle\Delta\alpha\rangle$) for each transition probed. In all cases, comparison of the properties of the aggregate species to those of the monomer allows the effects of excitonic coupling on the electronic properties of the dye to be examined.

A second property of interest is the number of dye molecules that are collectively excited when the aggregate absorbs light.¹⁴ One might expect this quantity, referred to here as N , to be less than the total number of chromophores in the aggregate because of the presence of inhomogeneities in the structure or environment or both that would limit delocalization of the exciton. Here, we obtain estimates of N for the J aggregates of $\text{DiSC}_{3+}(5)$ bound to polymeric DNA by comparison of the absorption line width of the monomer to that of the aggregate. As described below, comparison of the parameters obtained from electroabsorption spectroscopy of the aggregates to those of the monomer can also be used both to infer a value of N and to obtain additional information regarding the structure of the species.^{15,16}

Experimental Section

To form aggregates of $\text{DiSC}_{3+}(5)$ dyes, a poly(dI–dC) DNA duplex containing ~150–200 alternating inosine–cytosine base pairs was used. Inosine was used in place of the naturally occurring base guanine because the amino group of guanine protrudes toward the minor groove, sterically hindering the binding of the dyes.¹² The concentration of the dye was chosen to allow all of the potential binding sites (≥ 30) to be occupied. The aggregates form readily by allowing the solutions of DNA and the dye to mix for ~10 min. The Stark and steady-state fluorescence experiments on the aggregated species were performed in 35% ethylene glycol/5% methanol/water glass at 77 K in which the pH was maintained at 7.2 using a 10 mM phosphate buffer in the presence of 50 mM NaCl. The time-resolved fluorescence studies were performed at 10 °C in a solvent of 10 mM buffer at pH 7.1, 50 mM NaCl, and 10% methanol. Experiments on the monomer $\text{DiSC}_{3+}(5)$ were performed in ethylene glycol/methanol/water (80:10:10 by volume) in the absence of DNA.

Along with being necessary for the electroabsorption measurement, lowering the temperature of the sample from 298 to 77 K significantly increases the intensity of the J band. The sample cell was cooled by keeping it above the liquid nitrogen for ~10 min and then very slowly lowering it into the liquid nitrogen Dewar flask. This two-step process had the effect of minimizing the number of monomeric cyanine dyes present as judged by the absorption spectrum.

Instrumentation. The electroabsorption apparatus is home-built and has been previously described in detail.^{17,18} Steady-state fluorescence spectra were obtained using a Fluorolog-2 instrument (Spex) with 1 nm resolution. Time-resolved emission traces were obtained using a Timemaster fluorescence lifetime spectrometer (Photon Technology International). The instrument response for this system was measured to be 1.5 ± 0.1 ns.

Electroabsorption Data Analysis. The analysis of the electroabsorption data follows that in the literature.^{19,20} The equations shown here are appropriate for the experimental conditions used, i.e., the sample is isotropically embedded in a rigid glass. Essentially, the change in absorption due to the application of an external electric field is fit to the weighted sum of zeroth, first, and second derivatives of the zero-field absorption spectrum. The overall change in absorbance caused by the application of an electric field can be described by the following equation:

$\Delta A(\tilde{\nu}) =$

$$\vec{F}_{\text{eff}}^2 \left[\mathbf{a}_\chi A(\tilde{\nu}) + \mathbf{b}_\chi \frac{\tilde{\nu}}{15\hbar} \left\{ \frac{\partial}{\partial \tilde{\nu}} \left(\frac{A(\tilde{\nu})}{\tilde{\nu}} \right) \right\} + \mathbf{c}_\chi \frac{\tilde{\nu}}{30\hbar^2} \left\{ \frac{\partial^2}{\partial \tilde{\nu}^2} \left(\frac{A(\tilde{\nu})}{\tilde{\nu}} \right) \right\} \right] \quad (1)$$

The term $A(\tilde{\nu})$ represents the unperturbed absorption as a function of frequency ($\tilde{\nu}$), and \vec{F}_{eff} represents the field at the sample in V/cm. This effective field includes the enhancement of the applied field due to the cavity field of the matrix. The subscript χ represents the angle between the direction of the applied electric field and the electric field vector of the linearly polarized light. The experiments reported here are performed at $\chi = 54.7^\circ$ (magic angle). At $\chi = 54.7^\circ$, the expressions of \mathbf{a}_χ , \mathbf{b}_χ , and \mathbf{c}_χ are related to the change in the transition moment polarizability (A_{ij}) and hyperpolarizability (B_{ijj}), the change in the electronic polarizability ($\langle \Delta\alpha \rangle$), and the change in the dipole moments ($|\Delta\mu|$), respectively, as given in eqs 2–4.

$$\mathbf{a}_{54.7} = \frac{1}{3|m|^2} \sum_{ij} A_{ij}^2 + \frac{2}{3|m|^2} \sum_{ij} m_i B_{ijj} \quad (2)$$

$$\mathbf{b}_{54.7} = \frac{10}{|m|^2} \sum_{ij} m_i A_{ij} \Delta\mu_j + \frac{15}{2} \langle \Delta\alpha \rangle \quad (3)$$

$$\mathbf{c}_{54.7} = 5|\overline{\Delta\mu}|^2 \quad (4)$$

In this work, we quote $\langle \Delta\alpha \rangle$, which represents the average change in electronic polarizability between the ground and excited state (i.e., $\langle \Delta\alpha \rangle = 1/3 \text{tr}(\Delta\alpha)$). Information regarding $|\overline{\Delta\mu}|$ for the molecule is contained in the $\mathbf{c}_{54.7}$ term (eq 4). It is important to emphasize that, for an isotropic sample such as those studied in this work, only the magnitude and not the sign of $\overline{\Delta\mu}$ is measured. In the above equations, the tensors \underline{A} and \underline{B} represent the transition polarizability and hyperpolarizability, respectively. These describe the effect of \vec{F}_{eff} on the molecular transition moment: $\vec{m}(\vec{F}_{\text{eff}}) = \vec{m} + \underline{A} \cdot \vec{F}_{\text{eff}} + \vec{F}_{\text{eff}} \cdot \underline{B} \cdot \vec{F}_{\text{eff}}$. These terms are generally small for allowed transitions and can therefore be neglected relative to other terms in the expression for $\langle \Delta\alpha \rangle$ (eq 3), particularly in those species exhibiting a small value of $|\overline{\Delta\mu}|$, such as those reported here.

The coefficients, \mathbf{a}_χ , \mathbf{b}_χ , and \mathbf{c}_χ , are extracted by means of a linear least-squares (LLSQ) fit of the electroabsorption signal to the sum of the derivatives of $A(\tilde{\nu})$. If the resultant fit to the absorption line shape (a single set of \mathbf{a}_χ , \mathbf{b}_χ , and \mathbf{c}_χ) is *not* of high quality, this is an indication that there is more than one transition (electronic or vibronic) underlying the absorption band, each having different electrooptical properties. Our fitting strategies are described in ref 18.

Results and Discussion

Absorption Spectrum of DiSC₃₊(5) Monomer and H/J Aggregates. Figure 2 contains the absorption spectra of DiSC₃₊(5) monomer at 288 (panel a) and 77 K (panel b). The spectra in the presence of polymeric (~200 base pairs) duplex DNA at 278 (panel c) and at 77 K (panel d) are shown as well. The absorption spectrum arising from DiSC₃₊(5) changes dramatically in the presence of duplex DNA. At 278 K (Figure 2c), two peaks appear, one at ~600 nm (band i) and the second at ~750 nm (band iii) and there is a concomitant reduction in the absorption intensity due to the monomeric dye at ~660 nm (band ii). The red- and blue-shifted bands that appear in the

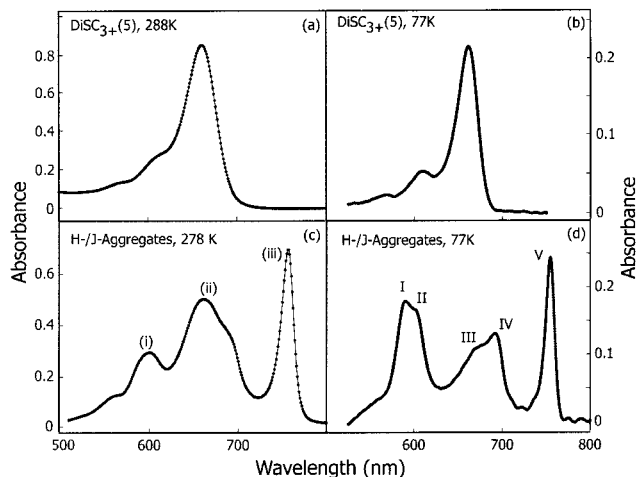


Figure 2. Absorption spectra of DiSC₃₊(5) monomers at (a) 288 and (b) 77 K in 80% ethylene glycol. Panel c shows the absorption spectrum of DiSC₃₊(5) at 278 K in the presence of duplex DNA. Bands are seen due to (i) H aggregates, (ii) residual monomer, and (iii) J aggregates. Panel d shows the absorption spectrum of DiSC₃₊(5) at 77 K in the presence of duplex DNA. Additional splittings are resolved in the H band (I and II) and the J band (IV and V). Residual monomer gives rise to transition III.

spectrum when DNA is added are assigned, respectively, to J- and H-type transitions of DiSC₃₊(5) aggregates bound to DNA.¹³

At 77 K, additional splittings are resolved in both the H bands (bands I and II in Figure 2d) and the J bands (bands IV and V in Figure 2d). These arise because of head-to-head interactions between adjacent dye dimers (γ_H and γ_J in Figure 1) and are roughly a factor of 4 larger for the J-type aggregate than for the H-type aggregate (Table 1). The primary splitting (β_J and β_H , Figure 1 and Table 1) that results from the stacking interaction between two cyanines within the minor groove (Table 1) is measured from the absorption maximum of the monomer to the midpoint of the two bands associated with the J band and H band, respectively. The value of β_H is 25% larger than that of β_J , suggesting that the face-to-face interactions in the H-aggregate structure are stronger than those in the J-aggregate structure.

The extremely narrow bandwidth of band V (fwhm $\approx 220 \text{ cm}^{-1}$) is a general characteristic of absorption spectra due to J aggregates. The fact that the higher-energy J-aggregate band in the absorption spectrum (band IV) is broader in appearance than the lower-energy band (band V) is in part due to overlap with residual monomeric cyanines (band III). Evidence for this overlap is also seen in the fluorescence emission spectrum obtained by excitation in this region as described below.

Theory¹⁰ predicts that the line width of the J band of the aggregate relative to that of the monomer scales as $N^{1/2}$. This effective reduction in the inhomogeneous line width is due to the averaging over multiple sites that occurs when the initial excitation is delocalized over the aggregate structure (motional averaging). For comparison to the line width of the J band, an estimate of $\sim 800 \text{ cm}^{-1}$ for the fwhm of the main vibronic feature ($\sim 660 \text{ nm}$) of the monomer absorption band at 77 K is obtained. This implies that N is ~ 16 , which is considerably larger than estimates by other methods described below.

Wiersma and co-workers previously found that line width measurements significantly overestimated the value of N compared to the results of photon echo experiments in studies of aggregates of pseudoisocyanine (PIC, Chart 1b), which is a dye somewhat similar in structure to DiSC₃₊(5).²¹ Their explanation for the discrepancy is that the inhomogeneous

TABLE 1: Spectroscopic Properties of Monomeric DiSC₃₊(5) and of H and J Aggregates Bound to DNA

DiSC ₃₊ (5) (77 K glass)	absorption maxima ^a (nm)	fluorescence maxima ^b (nm)	$2\beta^c$ (cm ⁻¹)	$2\gamma^c$ (cm ⁻¹)	$ \overline{\Delta\mu} $ (D)	$\langle\Delta\alpha\rangle$ (Å ³)
monomer	662	670			1.1 ± 0.1	-13 ± 2
H band	589, 602		3300	360	0.7 ± 0.05	-34 ± 4
J band	690, 754	759	2550	1200	0.6 ± 0.05	-74 ± 5

^a Errors are ± 2 nm. ^b Errors are ± 5 nm for the monomer and ± 1 nm for the J band. ^c 2β and 2γ are primary and secondary splittings, respectively (see Figure 1), reported in cm⁻¹ with errors of ± 150 cm⁻¹ each.

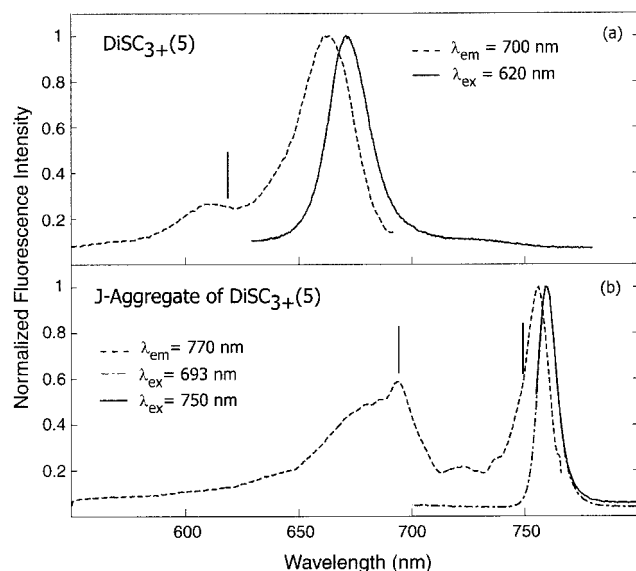


Figure 3. Fluorescence excitation (dashed line) and emission (solid line) spectra of DiSC₃₊(5) (a). The excitation spectrum was collected at 770 nm. Panel b shows the fluorescence excitation spectrum (dashed line) collected in the region of the J aggregate emission (750 nm). The emission spectra collected by exciting at 693 nm (dash-dot line) and at 750 nm (solid line) are also shown. Vertical bars indicate the excitation wavelengths used to obtain the emission spectra shown. All spectra were obtained at 77 K.

broadening of the monomeric dye has two sources, one being normal site broadening and the other being structural inhomogeneity due to small rotations of the quinoline rings. In contrast, the latter broadening mechanism should be minimized in the aggregate because of its stacked structure, while the site broadening would be roughly the same. They proposed that the site broadening of the monomer can be estimated instead by that measured for numerous other more rigid dyes in glasses (~ 300 cm⁻¹), and that *this* is a more reasonable value to compare to the line width of the J aggregate. Following this strategy yields values of N of between 2 and 4 for line widths of monomeric DiSC₃₊(5) chosen from 300 to 400 cm⁻¹, which is in better agreement with the other studies reported here.

Fluorescence Spectrum of the DiSC₃₊(5) Monomer and H/J Aggregates. The fluorescence spectrum of DiSC₃₊(5) at 77 K, monitored at 700 nm, is shown in Figure 3a. The Stokes shift between the excitation (dashed line) and emission (solid line) spectra is quite small (~ 180 cm⁻¹). Figure 3b contains the excitation (dashed line) and emission (solid line) spectra of the dyes bound to poly(dI-dC) DNA, also at 77 K. A significantly smaller Stokes shift (~ 90 cm⁻¹) is observed for the J-aggregate emission. As seen in the absorption spectra, the J-aggregate emission bands are roughly a factor of 4 narrower than that of the monomer. Not surprisingly, emission is very weak for excitation in the region of the H-aggregate absorption, and *no* structure is seen in the excitation spectrum that is reminiscent of the H-aggregate absorption band. Regarding the issue of whether the H and J bands arise from the same aggregate structure or from distinct aggregates that was raised

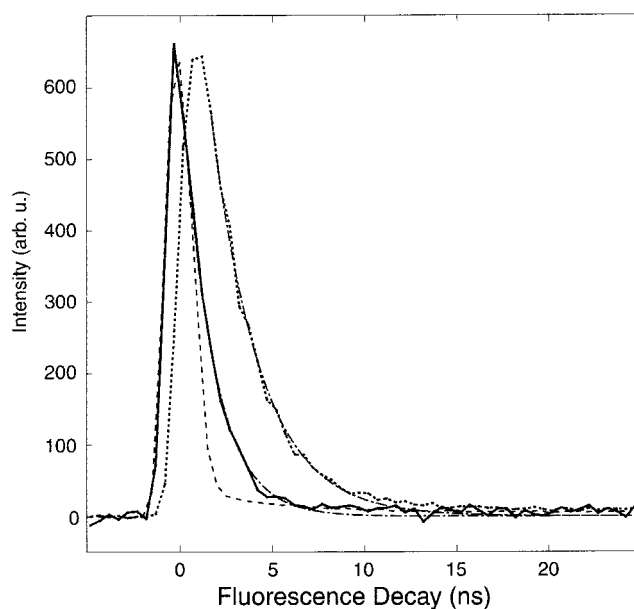


Figure 4. Decay curves of DiSC₃₊(5) monomer emission (dotted line) and J aggregate emission (solid line) obtained at 10 °C. The monomer was excited at 666 nm, and its emission was monitored at 678 nm. The J aggregates were excited at 695 nm, and their emission was monitored at 750 nm. The spectra represent the average of 10 scans. The fit to each curve is shown as dashed-dot lines, and the instrument response function is shown in the dashed line.

earlier in the Introduction, this result supports the second possibility, at least for the temperature and solvents used in this study.

Excitation into the broad transition centered at 675 nm produces emission both in the region of the J-band emission and in the region of that from the monomer, particularly if the latter is present in excess (not shown). Again, this suggests that the feature arises from an overlap of the upper J-band transition and monomeric dye molecules either free or bound to the DNA. It is also quite possible that excitation of monomeric dye that is bound to the DNA results in energy transfer to the J aggregate thereby giving rise to J-type emission.

Fluorescence Lifetime Measurements. The fluorescence decay curves of the J aggregate (solid line) and of DiSC₃₊(5) monomer (dotted line) obtained at 10 °C are shown in Figure 4 along with the response function of the spectrometer (dashed line). It is evident from the figure that the decay of the aggregate emission is more rapid than that of the monomer. Both curves were deconvolved from the instrument response function and fit to a single-exponential decay curve (dashed-dot lines). This yielded a time constant of 2.5 ± 0.1 ns for the monomer and 1.5 ± 0.1 ns for the aggregate. Though the decay time of the aggregate is essentially equal to the measured response function (1.5 ± 0.1 ns), its emission decay curve is clearly distinguishable from the instrument profile.

The radiative rate of the aggregate is predicted to be N times faster than that of the monomer. Therefore, *if* the nonradiative rates of the monomer are unchanged on formation of the

aggregate, the measured fluorescence decay rate of the aggregate should obey the same relationship.⁶ Here, we observe a factor of ~ 1.7 decrease in the fluorescence lifetime on aggregate formation, implying a value of N close to 2.

There are several limitations to this estimate of N . First, while the increase in the fluorescence decay rate of DiSC₃₊₍₅₎ on formation of the J aggregate follows the expected trend, there is the possibility that the lifetime of the aggregate emission is overestimated because of the time resolution of the instrument used. If the aggregate emission is multiexponential, any decay components shorter than the response function would not be observable in the data. A second limitation is the relatively high temperature used, which was dictated by the instrument design. Lowering the temperature should reduce the contributions from nonradiative processes to the fluorescence decay rates of both the monomer and the aggregate, thereby producing a better estimate of N . To address these issues, experiments at lower temperatures and with higher time resolution as well as measurements of the emission yields are planned soon.

Electroabsorption Spectra of DiSC₃₊₍₅₎ Monomer and H/J Aggregates. To establish a point of comparison for understanding the electronic properties of the aggregates, we measured the electroabsorption spectrum of DiSC₃₊₍₅₎. Figure 5 shows the absorption (panel a) and the electroabsorption (panel b) spectra (solid line) and the fit (dashed line) to the Stark signal for DiSC₃₊₍₅₎ at 77 K. The high quality of the fit suggests that the monomer is exclusively formed under these conditions, and the values of $|\overline{\Delta\mu}|$ and $\langle\Delta\alpha\rangle$ are reported in Table 1. Negative values of $\langle\Delta\alpha\rangle$, such as those measured here for DiSC₃₊₍₅₎, have previously been reported for other cyanine dyes.²²

Turning now to the aggregate species, the absorption spectrum and the electroabsorption (solid line) and fit (dashed-dot line) of H and J aggregates of DiSC₃₊₍₅₎ are contained in Figure 5, panels c and d, respectively. For both species, the quality of fits of the electroabsorption spectrum to derivatives of the absorption spectrum is remarkably good, suggesting that use of the DNA template leads to aggregates with highly uniform properties (minimal heterogeneity) as measured by their field response. In contrast, the signal in the region corresponding to bands III and IV in Figure 5d could not be fit because, as stated earlier, it arises from two overlapping signals. Because of this overlap, all parameters reported for the J aggregate are derived from the fit to band V alone.

The H and J aggregates exhibit nearly identical values of $|\overline{\Delta\mu}|$ (~ 0.6 – 0.7 D), though $\langle\Delta\alpha\rangle$ for the J aggregates (-74 Å³) is twice that of the H aggregates (-34 Å³). For comparison, the values of $|\overline{\Delta\mu}|$ and $\langle\Delta\alpha\rangle$ for the monomer are 1.1 D and -13 Å³, respectively. Note that the local field appropriate to the environment of the monomer may be different than that for the aggregate because the former is surrounded by a polar glass while the latter sees the environment of the DNA minor groove (see Experimental Section) and that this could somewhat affect the comparison between their associated $|\overline{\Delta\mu}|$ and $\langle\Delta\alpha\rangle$ values. While the dielectric properties of the DNA environment are a topic of current research, the binding site may be nonpolar because of the presence of the aromatic bases.

In the paragraphs following, we first outline the implications of these results regarding the structure and strength of the electronic coupling within the aggregates and compare to other published studies. Next, we justify the appropriateness of the Liptay model to analyze the field response of our aggregates, in part on the basis of this comparison. Finally, we compare the values of N for the J aggregates that are inferred from the

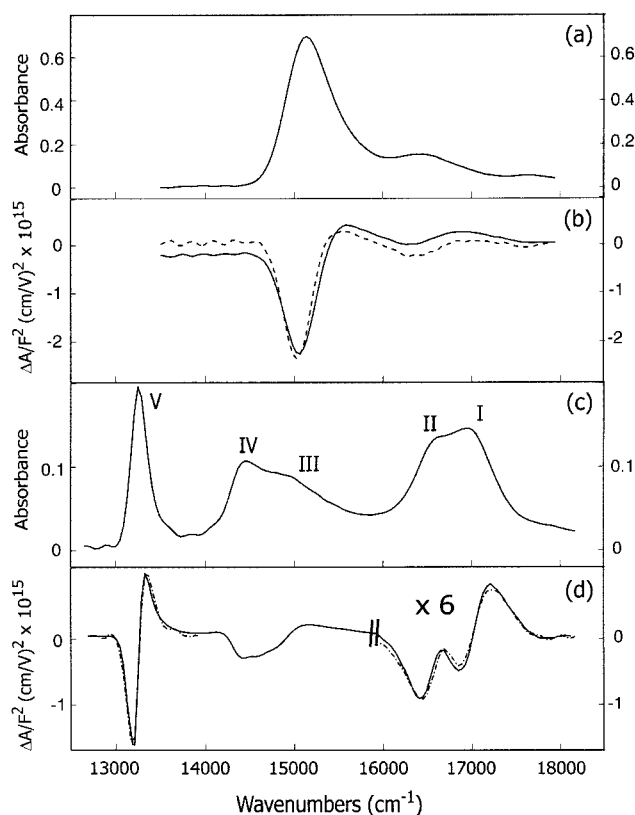


Figure 5. Absorption band of monomeric DiSC₃₊₍₅₎ in ethylene glycol/methanol/water (80:10:10) glass at 77 K (a), electroabsorption (solid line) spectrum of DiSC₃₊₍₅₎ and fit (dashed line) (b), and absorption spectrum of DiSC₃₊₍₅₎ in the presence of polymeric (~ 200 base pairs) duplex poly(dI–dC) DNA in a 77 K glass consisting of 35% ethylene glycol, 60% NaPi buffer (pH=7.1) and 5% methanol (c). The labeling of the peaks (I–V) is explained in Figure 2. Panel d shows the electroabsorption (solid line) and fit (dashed-dot line) to the J-band region (peak V) and the H-band region (peaks I and II) of the aggregate spectrum. These two regions of the spectrum were fit separately and the values obtained are in Table 1. Note that the signal in the H-band region is multiplied by a factor of 6. The feature in the central region (bands III and IV) was not fit because it consists of overlapping transitions (see text).

various measurements presented here and suggest further directions for this work.

Following the literature, we can associate the ratio of $\langle\Delta\alpha\rangle$ of both the H and J aggregates to that of the monomer with the value of N upon optical excitation.¹⁵ The magnitude of $\langle\Delta\alpha\rangle$ for the H aggregates (34 Å³) is roughly twice that of the DiSC₃₊₍₅₎ monomer, implying that the excitation is delocalized over two chromophores in the aggregate. This is expected because of the strong face-to-face interaction of the two monomers in the H aggregates that is also evident in the large value of β_H . The relatively small value of γ_H , in turn, is consistent with the picture that electronic couplings with chromophores beyond the two composing the dimer are significantly weaker.

For the J aggregates, we observe a much larger $\langle\Delta\alpha\rangle$ (74 Å³) suggesting that at least 4–6 dye molecules are strongly coupled. This is consistent with the large head-to-head interaction implied by the measured value of γ_J . One reason that the extent of delocalization is apparently larger in the J aggregate may simply be that each dye interacts with a minimum of two of its neighbors to form the proposed J-type brickwork structure (see Figure 1). In contrast, because, in H aggregates, the dyes are thought to stack in register (see Figure 1), interactions with adjoining dyes may be weaker.

Regarding the measured $|\overline{\Delta\mu}|$ values for the H and J aggregates, they are quite similar and both are somewhat smaller than that of the monomer. This is as expected from eq 5, derived in ref 16.

$$\cos \theta = \frac{|\overline{\Delta\mu_A}|}{|\overline{\Delta\mu_M}|} \quad (5)$$

Here, the subscripts A and M refer to the aggregate and the monomer, respectively, and θ is the angle between the $\overline{\Delta\mu}$ vectors of the constituent dye monomers in the aggregate. Note that eq 5 predicts that the *maximum* value of $|\overline{\Delta\mu}|$ for an aggregate is that of the monomer, observed if the $\overline{\Delta\mu}$ vectors of the constituent dyes are all parallel ($\cos \theta = 1$).

Interestingly, very large values of $|\overline{\Delta\mu}|$, even in nominally symmetric aggregate structures, have been reported in the literature. These have been attributed to large asymmetric matrix or protein fields interacting with a highly polarizable aggregate²³ and field-induced displacement of associated counterions.²⁴ Neither factor appears to be important for the aggregates studied here judging by the similarity of their $|\overline{\Delta\mu}|$ values to that of DiSC₃₊(5) itself.

Likewise, a lower value of $\langle\Delta\alpha\rangle$ is measured for the J aggregates studied here than for many other types of aggregates formed that have been studied (for comparison, note that we report $\langle\Delta\alpha\rangle$, which is the *average* value of $\Delta\alpha$ while $\text{tr}(\Delta\alpha)$ is sometimes reported).^{15,25,26} For example, Misawa et al. measured $\sim 18 \times 10^3 \text{ \AA}$ for $\text{tr}(\Delta\alpha)$ of oriented J aggregates of PIC formed by vertical spin coating.²⁶ Because the $\langle\Delta\alpha\rangle$ values obtained for aggregates formed by the DNA templating method are significantly smaller than those reported for aggregates of other chromophores, we surmise that the species studied here are smaller or that their constituent chromophores are more weakly coupled or both. Future experiments using oligomeric DNA to form aggregates of better-defined size will help to sort out these possibilities. It will also be useful to vary the identity of the bound dye, if that proves possible.

In addition to the factors outlined above, a breakdown of the Liptay formalism (eqs 1–4) has also been invoked to explain the measurement of $\langle\Delta\alpha\rangle$ or $|\overline{\Delta\mu}|$ values or both in the aggregate that are many times larger than those seen in the monomer. This method of analysis makes the assumption that the transition frequencies of the system being probed are more widely separated than the homogeneous line widths (i.e., the limit of large inhomogeneous broadening). For strongly coupled systems, this could break down as discussed by Mukamel et al.²⁵ A second possibility is that the applied field strongly stabilizes charge-transfer excited states, which are present in the aggregate but not in the monomer. This would increase $\langle\Delta\alpha\rangle$ by preferentially enhancing the polarizability of the final state in the absorption because of their proximity in energy.²⁵ Similarly, field-induced mixing of such charge-transfer states into the excited state could increase the excited state's dipole moment, while the ground state remains nonpolar.²⁷ In the latter cases, one cannot think of the field as merely perturbing the energies of the electronic states but as altering their character.

Because the results obtained for $\langle\Delta\alpha\rangle$ and $|\overline{\Delta\mu}|$ in the aggregates studied here appear to scale in a reasonable manner with those of the monomer, we presume that the effects described above do not obtain though, again, a more rigorous analysis awaits the development of aggregates for which we have a better estimate of the number of chromophores.

Summary and Conclusions

We have presented a number of photophysical studies characterizing the electronic properties of novel H and J aggregates of the cyanine dye DiSC₃₊(5) formed by noncovalent binding to polymeric DNA. Estimates based on the line widths and fluorescence decay rates of the J aggregate compared to those of the monomer suggest that the number of dye chromophores that are coherently coupled on excitation (N) in the aggregate is between 2 and 4. Electroabsorption studies on the J- and H-aggregate bands suggest that the aggregates formed are quite uniform in terms of their electronic properties as judged by the high quality of the fits obtained. Comparison of the measured polarizabilities ($\langle\Delta\alpha\rangle$) of the aggregates with that of the monomer suggests that N is somewhat larger (~ 4 – 6) for the J aggregate than for the H aggregate (~ 2). This is consistent with the larger head-to-head couplings for the former that are inferred from the splittings in the absorption spectra.

Acknowledgment. This work was supported by the NSF through the CAREER and POWRE programs. We also thank Drs. Bruce Armitage, David Yaron, and Frank Spano for useful discussions and Miaomiao Wang and Isil Dilek for help in forming the DNA–dye aggregates. We also acknowledge the Center for Molecular Analysis at CMU for use of the absorption spectrometer and Dr. Armitage for use of the fluorescence lifetime spectrometer.

References and Notes

- (1) Mukamel, S.; Chemla, D. S., Eds. Special Issue on Confined Excitations in Molecular and Semiconductor Nanostructures. *Chem. Phys.* **1996**, *210*.
- (2) Special Issue on Light-Harvesting Physics *J. Phys. Chem. B* **1997**, *101*.
- (3) Gilman, P. B. *J. Photogr. Sci. Eng.* **1974**, *18*, 418–430.
- (4) Wang, Y. *Chem. Phys. Lett.* **1986**, *126*, 209–214.
- (5) Fidler, H.; Knoester, J.; Wiersma, D. A. *Chem. Phys. Lett.* **1990**, *171*, 529–536.
- (6) Spano, F. C.; Kuklinksi, J. R.; Mukamel, S. *J. Chem. Phys.* **1991**, *94*, 7534–7544.
- (7) Ozelik, S.; Akins, D. L. *J. Phys. Chem. B* **1997**, *101*, 3021–3024.
- (8) Potma, E. O.; Wiersma, D. A. *J. Chem. Phys.* **1998**, *108*, 4894–4903.
- (9) Lidzey, D. G.; Bradley, D. D. C.; Virgili, T.; Armitage, A.; Skolnick, M. S.; Walker, S. *Phys. Rev. Lett.* **1999**, *82*, 3316–3319.
- (10) Knapp, E. W. *Chem. Phys.* **1984**, *85*, 73–82.
- (11) Ishimoto, C.; Tomimuro, H.; Seto, J. *Appl. Phys. Lett.* **1986**, *49*, 1677–1679.
- (12) Seifert, J. L.; Connor, R. E.; Kushon, S. A.; Wang, M.; Armitage, B. A. *J. Am. Chem. Soc.* **1999**, *121*, 2987–2995.
- (13) Wang, M.; Silva, G. L.; Armitage, B. A. *J. Am. Chem. Soc.* **2000**, *122*, 9977–9986.
- (14) Mobius, D.; Kuhn, H. *Isr. J. Chem.* **1979**, *18*, 375–384.
- (15) Friedrich, J.; Wendt, H. *Chem. Phys.* **1996**, *210*, 101–107.
- (16) Dubinin, N. V. *Opt. Spectrosc. (Transl. of Opt. Spektrosk.)* **1977**, *43*, 49–51.
- (17) Locknar, S. A.; Peteanu, L. A. *J. Phys. Chem. B* **1997**, *102*, 4240–4246.
- (18) Premvardhan, L. L.; Peteanu, L. A. *J. Phys. Chem. A* **1999**, *103*, 7506–7514.
- (19) Liptay, W. Dipole Moments and Polarizabilities of Molecules in Excited Electronic States. In *Excited States*; Lim, E. C., Ed.; Academic Press: New York, 1974; pp 129–229.
- (20) Bublitz, G. U.; Boxer, S. G. *Annu. Rev. Phys. Chem.* **1997**, *48*, 213–242.
- (21) De Boer, S.; Vink, K. J.; Wiersma, D. A. *Chem. Phys. Lett.* **1987**, *137*, 99–106.
- (22) Bublitz, G. U.; Ortiz, R.; Marder, S. R.; Boxer, S. G. *J. Am. Chem. Soc.* **1997**, *119*, 3365–3376.
- (23) Middendorf, T. R.; Mazzola, L. T.; Lao, K.; Steffen, M. A.; Boxer, S. G. *Biochim. Biophys. Acta* **1993**, *1143*, 223–234.
- (24) Misawa, K.; Minoshima, K.; Ono, H.; Kobayashi, T. *Chem. Phys. Lett.* **1994**, *220*, 251–256.
- (25) Somsen, O. J. G.; Chernyak, V.; Frese, R. N.; van Grondelle, R.; Mukamel, S. *J. Phys. Chem. B* **1998**, *102*, 8893–8908.
- (26) Misawa, K.; Kobayashi, T. *Nonlinear Opt.* **1995**, *14*, 103–120.
- (27) Gottfried, D. S.; Boxer, S. G. *J. Lumin.* **1992**, *51*, 39–50.